References and Notes

1. E. L. Knudsen, M. Konishi, *Science* **200**, 795 (1978).
2. A. Moiseff, M. Konishi, *J. Neurosci.* **3**, 2553 (1983).
3. W. E. Sullivan, M. Konishi, *J. Neurosci.* **4**, 1786 (1984).
4. T. T. Takahashi, A. Moiseff, M. Konishi, *J. Neurosci.* **4**, 1781 (1984).
5. Data were obtained from 14 adult barn owls (Tyto alba) of both sexes. Owls were anesthetized by initial intramuscular injections of ketamine hydrochloride (25 mg/kg; Ketaset, Fort Dodge) and diazepam (1.3 mg/kg; Western Medical Supply, Phoenix, AZ). Sharp glass electrodes filled with 2% neurobiotin in 2 M potassium acetate (pH 7.4) were advanced under visual control through a hole made on the bony cap containing the optic lobe. In all experiments, acoustic stimuli, broadband noise 100 ms in duration, 30 dB above threshold were delivered by an earphone assembly consisting of a Knowles ED-1914 receiver as a sound source, a Knowles BF-1743 damped coupling assembly for smoothing the frequency response of the receiver, and a calibrated Knowles 1939 microphone for monitoring sound pressure levels in the ear canal. Neural signals were amplified with an Axoclamp-2A intracellular amplifier, digitized, and stored by a computer at a sampling rate of 24 kHz. To visualize and measure synaptic potentials, we removed spikes using a median filter method (*6*). For more detailed methods, see (*7*).
6. B. Jagadeesh, H. S. Wheat, L. L. Kontsevich, C. W. Tyler, D. Ferster, *J. Neurophysiol.* **78**, 2772 (1997).
7. J. L. Peña, M. Konishi, *Proc. Natl. Acad. Sci. U.S.A.* **97**, 11787 (2000).
8. We could show that postsynaptic inhibitory potentials caused hyperpolarization, because we could reverse them by changing the membrane potential. However, because sound-evoked synaptic potentials often contained a mixture or balance of excitatory and inhibitory postsynaptic potentials, we refer to them as depolarizing and hyperpolarizing postsynaptic potentials, respectively.
9. E. I. Knudsen, M. Konishi, *Science* **202**, 778 (1978).
10. G. H. Golub, C. F. Van Loan, *Matrix Computations* (Johns Hopkins Univ. Press, Baltimore, MD, 1989).
11. Sound-induced mean spike rates or postsynaptic potentials plotted against ITD and ILD are referred to as ITD and ILD curves, respectively. To make an ITD or ILD curve, we kept one of the two inputs constant at its best value (referred to as best ILD and ITD). Space-specific neurons may respond to an ITD and ITD $\pm$ *T*, where *T* is either the period of the stimulus tone or the inverse of the best frequency of the neuron (*7*).
12. The confidence limits are $\lambda \pm p_t\sigma/n^{1/2}$, where λ is the first singular values, p_t is a student random variable that varies with the confidence interval chosen and $n - 1$ degrees of freedom, σ is the standard deviation of the mean membrane potential, and n is the number of stimulus repetitions. The term $p_t\sigma/n^{1/2}$ represents the variability (noise) in the data.
13. T. Poggio, *Cold Spring Harbor Symp. Quant. Biol.* **55**, 944 (1990).
14. A. Pouget, T. J. Sejnowski, *J. Cognit. Neurosci.* **9**, 222 (1997).
15. E. Salinas, L. F. Abbott, *Proc. Natl. Acad. Sci. U.S.A.* **93**, 11956 (1996).
16. C. Koch, *Biophysics of Computation* (Oxford Univ. Press, Oxford, 1998).
17. R. A. Andersen, L. H. Snyder, D. C. Bradley, J. Xing, *Annu. Rev. Neurosci.* **20**, 303 (1997).
18. N. Hatsopoulos, F. Gabbiani, G. Laurent, *Science* **270**, 1000 (1995).
19. H. J. Sun, B. J. Frost, *Nature Neurosci.* **1**, 296 (1998).
20. M. Egelhaaf, A. Borst, W. Reichardt, *J. Opt. Soc. Am. A* **6**, 1070 (1989).
21. W. R. Taylor, S. He, W. R. Levick, D. I. Vaney, *Science* **289**, 2347 (2000).
22. B. W. Mel, C. Koch, in *Advances in Neural Information Processing Systems*, vol. 2, D. S. Touretzky, Ed. (Kaufmann, San Mateo, CA, 1990), pp. 474–481.
23. I. Fujita, M. Konishi, *J. Neurosci.* **11**, 722 (1991).
24. D. E. Feldman, E. I. Knudsen, *J. Neurosci.* **14**, 5939 (1994).

25. We thank P. Mitra and F. Gabbiani for their advice on using the svd, G. Kreiman and B. Christianson for their help with mathematics, C. Koch and G. Laurent for their enthusiasm and criticisms, C. Malek for computer matters, and G. Akutagawa for histology. This work was supported by NIH grant DC00134.

22 January 2001; accepted 9 March 2001

Josephson Junctions with Tunable Weak Links

Jan Hendrik Schön,[1]* Christian Kloc,[1] Harold Y. Hwang,[1] Bertram Batlogg[1,2]

The electrical properties of organic molecular crystals, such as polyacenes or C_{60}, can be tuned from insulating to superconducting by application of an electric field. By structuring the gate electrode of such a field-effect switch, the charge carrier density, and therefore also the superfluid density, can be modulated. Hence, weak links that behave like Josephson junctions can be fabricated between two superconducting regions. The coupling between the superconducting regions can be tuned and controlled over a wide range by the applied gate bias. Such devices might be used in superconducting circuits, and they are a useful scientific tool to study superconducting material parameters, such as the superconducting gap, as a function of carrier concentration or transition temperature.

Superconductivity is a most intriguing macroscopic quantum state, known for almost a century (*1*), yet still of great intellectual challenge and attraction, even as new classes of materials and new pairing mechanisms and order parameter symmetries are discovered. A particular consequence of the macroscopic quantum state is the occurrence of the Josephson effect when two superconductors are weakly connected. This effect is at the heart of practical devices such as ultrasensitive magnetic field detectors. In these devices, a carefully crafted thin insulating layer typically provides the coupling between superconductors. The coupling strength is exponentially sensitive to the insulator thickness and is fixed once the junction has been fabricated. However, it would be desirable to have an adjustable link, both in single-junction devices or in circuits where many superconductors could be Josephson-coupled and decoupled in an externally controlled way, as might be needed in quantum computing. We describe a method to create Josephson junctions where the coupling strength between two superconductors can be varied over the full possible range simply through the variation of an external voltage. It is based on the idea of controlling the superconducting properties of materials by an applied electric field (*2*). Such modulation has been demonstrated in a variety of field-effect devices (*3*–*9*). The technique of gate-induced superconductivity was used to exploit the capability of creating a controlled spatial modulation of the superfluid density within the same material through a suitable modification of the gate potential profile. Hence, an external

[1]Bell Laboratories, Lucent Technologies, 600 Mountain Avenue, Murray Hill, NJ 07974–0636, USA. [2]Solid State Physics Laboratory, ETH Hönggerberg, CH-8093 Zürich, Switzerland.

*To whom correspondence should be addressed. E-mail: hendrik@lucent.com

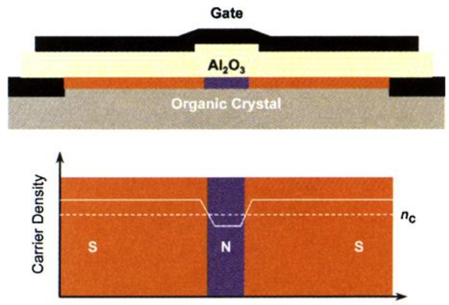

Fig. 1. Schematic of a "weak link" prepared on an organic single crystal. The cross-section of such a weak link shows the structured gate dielectric layer. By adjusting the gate voltage, a spatial variation of the carrier concentration can be achieved, which leads to the formation of a weak link [superconductor–normal conductor–superconductor (SNS) structure], although the details depend sensitively on the gate voltage, as seen in the insets of Fig. 3. Rather than forming a normal conducting region, a nonconducting (insulating) region appears to form.

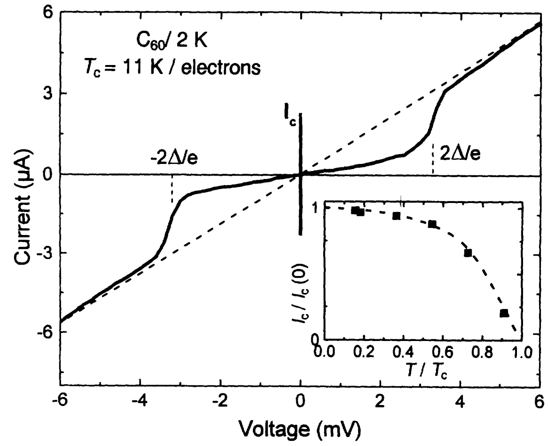

Fig. 2. Current-voltage characteristic of an electron-doped C_{60} Josephson junction at 2 K. The inset shows the temperature dependence of the critical Josephson current I_c.

voltage controls the carrier density and width of a normal conducting region, resulting in a modulation of the coupling strength between the two adjacent superconductors. We have produced tunable weak links in a series of organic compounds, including polyacenes and fullerenes. Controllable weak links have been demonstrated using superconducting metal electrodes in inorganic semiconductor field-effect structures (*10–12*). In addition, we determined the superconducting gap Δ from the current-voltage (*I-V*) characteristics of such devices for transition temperatures T_c ranging from 2 to 52 K. For hole-doped C_{60}, T_c has been varied from 7 to 52 K. The ratio of $2\Delta/k_BT_c$ varies between 3.3 and 3.8, indicating weak to intermediate coupling strength of the organic superconductors.

Molecular crystals of anthracene, tetracene, pentacene, and C_{60} were grown from the vapor phase in a stream of hydrogen (*13*). Field-effect transistors were prepared on cleaved crystal surfaces (*14*) using gold electrodes and an insulating Al_2O_3 layer (50 to 100 nm thick). Although all single crystal–based field-effect devices that were investigated showed ambipolar activity (*15*), electron, as well as hole, superconductivity was only observed in C_{60}. The mobilities at low temperatures and at the high carrier concentrations are in the range from 1 to 100 cm^2 V^{-1} s^{-1}. The corresponding mean free path is in the range of several nm. The critical temperatures ranged from 2 K in pentacene (*7*) to 52 K in hole-doped C_{60} (*9*). Josephson junctions (*16*) were prepared by creating a narrow region of a thicker gate dielectric layer. This was achieved by evaporating source- and drain-electrodes (gold or aluminum), and by sputtering of a first uniform layer of the gate dielectric (Al_2O_3). Then, shallow-angle shadow-mask evaporation was used to deposit the part of the gate electrode, leaving a gap of >50 nm. An additional 25 to 75 nm Al_2O_3 layer was deposited on top of the gapped electrode, followed by deposition of a second gate layer, which is connected to the first gate layer. As a result, the electric field under the narrow, thicker part of the gate oxide is reduced and the carrier concentration in the channel region exhibits a spatial variation (Fig. 1). Details of the field and carrier profile will have to be investigated in a further study. As the gate voltage increased, the carrier concentration increases, but is suppressed under the ridge of the gate dielectric. At a certain threshold voltage, superconductivity is induced underneath the two thinner parts of the dielectric layer. Upon further increase of the

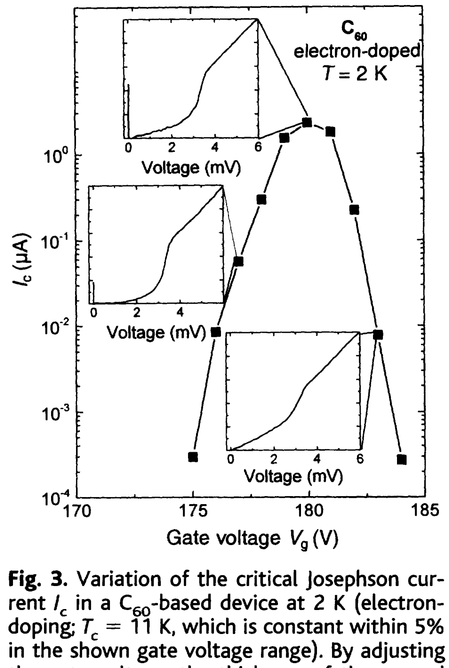

Fig. 3. Variation of the critical Josephson current I_c in a C_{60}-based device at 2 K (electron-doping; T_c = 11 K, which is constant within 5% in the shown gate voltage range). By adjusting the gate voltage, the thickness of the normal conducting region can be varied, giving rise to a modulation of I_c. The critical Josephson current is normalized to the maximum I_c obtained for this junction (V_g = 180 V). The insets show the current-voltage characteristics for different gate voltages (the current is normalized to the value at 6 mV).

gate voltage V_g, the two sides are Josephson coupled and a supercurrent flows at zero bias between source and drain. A priori, it is difficult to predict whether the weak link is of superconductor–normal metal–superconductor (SNS) or of superconductor-insulator-superconductor (SIS) type. Obviously, in the present experiments, a high gate voltage is necessary to induce superconductivity and then an additional variation by a few volts is needed to tune the coupling strength. In such a device, no voltage gain can be achieved.

Such a *I-V* characteristic for a C_{60} (electron-doped) Josephson junction is shown at 2 K (Fig. 2). The transition temperature of electron-doped C_{60} is 11 K. Similar characteristics have been observed for the other materials, and we did not observe any systematic differences between polyacenes and C_{60}, despite their different superconducting coherence lengths (30 to 100 Å). As we discuss later, however, the *I-V* characteristics depend on the tuning voltage. The current at zero voltage represents the critical Josephson current I_c, which is given by the maximum amount of current that the tunneling Cooper pairs can carry (Fig. 2). In order to investigate the microscopic nature of the weak link, further experiments will be needed. The tunneling characteristics reveal a nonideal junction with rather high transparency (Figs. 2 and 3) (*17*). The transparency increases with increasing gate voltage, which might be explained by the increased density of charge carriers under the ridge. Hence, the devices first resemble SIS junctions, and at higher voltages, change over to more SNS-type behavior.

In addition, the preparation of Josephson junctions with gate-induced superconductors allows the adjustment of the

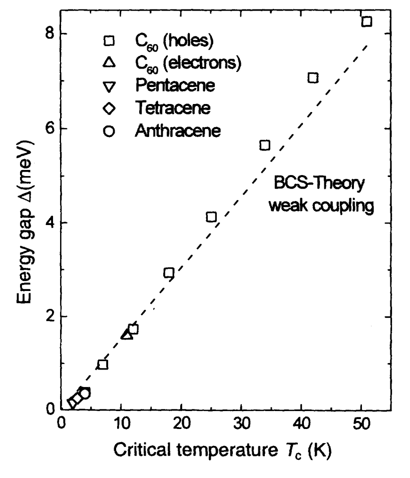

Fig. 4. Dependence of the superconducting gap Δ as a function of the critical temperature T_c, revealing a linear dependence. The slope is slightly higher than predicted in the Bardeen-Cooper-Schrieffer (BCS) weak coupling limit.

strength of the weak link by the applied gate bias. Because the gate bias controls the carrier concentration in the channel, the width of the normal or nonconducting region (Fig. 1), as well as the coherence length, can be adjusted by the applied gate bias. Consequently, the strength of the weak link, which depends on both parameters, the width, and the coherence length (*18*), can be modified in a controlled way. The critical Josephson current and the properties of the junction can then be controlled precisely over a wide range (Fig. 3). Gate-controlled supercurrents have also been achieved in a variety of metal-inorganic semiconductor (*10–12*) and high-T_c superconductor devices (*4*). Our approach is different in that the same material acts as superconductor and normal conductor/insulator simply by the variation of the carrier density. By using two (or more) gate electrodes, the Josephson coupling between gate-induced superconductors might be refined.

The strength of the Josephson coupling varies rather rapidly as the gate voltage is ramped up (Fig. 3). The magnitude of the Josephson current I_c increases with V_g, reaches a maximum, and then drops quickly again. The details, however, depend on several factors, including the gate capacitance profile (given by the gate oxide thickness) and the electronic properties of the superconductor, such as the carrier concentration dependence of T_c, and the superconducting coherence length. In all the various junctions, we find similar $I_c(V_g)$ dependencies, i.e., a strong variation of I_c within a few percent of V_g. The temperature dependence of I_c is shown in the inset of Fig. 2. The rapidly changing character of the junction is also evident from the junction resistance, decreasing from ~20 kilohms at V_g = 177 V to ~1 kilohms at maximum I_c (at 180 V).

The junction geometry used to study Josephson coupling also offers the opportunity to measure the superconducting gap Δ and its dependence on the carrier density, i.e., T_c. Because such investigations can be performed on the same device, the effects of additional disorder or structural changes due to chemical doping of the sample are eliminated. If the applied voltage exceeds the energy 2Δ to break the Cooper pairs, the current through the junction is carried by quasiparticles. In Figs. 2 and 3, we show several current-voltage characteristics, measured at 2 K in electron-doped C_{60}, for an electron concentration that results in a T_c of 11 K. Although the current is not zero below the gap voltage, the value of the gap Δ can nevertheless be clearly discerned by inspection of the derivative (dI/dV).

The experiments for different materials followed different protocols. For materials with low T_c, we measured the *I-V* characteristics at 1.7 K. Thus, the experimentally deduced values of Δ are reduced compared to $\Delta(T \rightarrow 0)$, especially for polyacene crystals. However, $\Delta(T \rightarrow 0)$ can be estimated from the temperature dependence of Δ (*19*). For C_{60}, we applied gate voltages over a wide range, resulting in a variation of T_c up to 11 K for electron-doping and up to 52 K for hole-doping. Then, we measured the *I-V* characteristics at several fixed gate voltages as a function of temperature in order to determine $\Delta(T,V_g)$, thereby calibrating the full T_c dependence on the gate bias. For other gate voltages, T_c is deduced from the previously measured $T_c(V_g)$ (*9*). Figure 4 shows an almost linear dependence of Δ on T_c. More insight is gained by plotting $2\Delta/k_BT_c$ versus T_c (Fig. 5). The experimental values for this ratio vary between 3.3 and 3.8, which is within the considerable experimental uncertainties consistent with weak to intermediate strong coupling [$2\Delta(0) = 3.52 \cdot k_BT_c$] (*19*). Because the subgap current was larger in C_{60} junctions with the highest T_c, Δ might be slightly overestimated.

The demonstration that Josephson junctions with tunable weak links can be fabricated for materials exhibiting gate-induced superconductivity opens up possibilities for scientific research as well as superconducting electronic circuits. The control of the superconducting and junction properties by an applied voltage might be useful in the fabrication of circuits for superconducting electronics or Josephson junction arrays. For example, the use of Josephson junction arrays as qubits has been demonstrated, which are suitable for scaling to large numbers of devices (*20–22*). However, at this point it is difficult to use standard lithographic processes on top of the molecular crystals without modifying their properties. Therefore, the use of a bottom-gate field-effect device instead of the top-gate configuration will facilitate the implementation of such tunable weak links and more complex circuitry because the gate structures can be defined by standard lithography. It has recently been demonstrated that large-scale integration of organic electronic devices on prepatterned Si circuitry is possible (*23*).

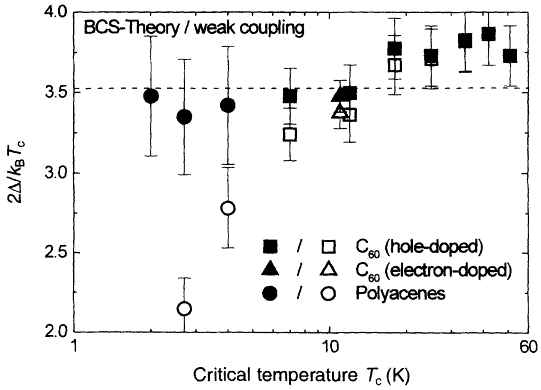

Fig. 5. Ratio of the superconducting gap Δ and the transition temperature T_c as a function of T_c for the various investigated organic materials. The open symbols are the experimental data for the gap at the measurement temperature $\Delta(T)$ and the solid symbols are the estimation of the zero temperature gap $\Delta(T \rightarrow 0)$. The observed values are in reasonable accordance with the weak coupling limit of the BCS theory ($2\Delta = 3.52 \cdot k_BT_c$).

References and Notes

1. H. K. Onnes, *Leiden Commun.* **1206**, 1226 (1911).
2. R. E. Glover, M. D. Sherill, *Phys. Rev. Lett.* **5**, 248 (1960).
3. T. M. Klapwijk, D. R. Heslinga, W. M. van Huffelen, in *Superconducting Electronics*, H. Weinstock, M. Nisenoff, Eds. (Springer, Berlin, 1989), pp. 385–408.
4. J. Mannhart, *Semicond. Sci. Technol.* **9**, 49 (1996).
5. C. H. Ahn *et al.*, *Science* **284**, 1152 (1999).
6. J. H. Schön, Ch. Kloc, R. C. Haddon, B. Batlogg, *Science* **288**, 656 (2000).
7. J. H. Schön, Ch. Kloc, B. Batlogg, *Nature* **406**, 704 (2000).
8. ______, *Nature* **408**, 549 (2000).
9. J. H. Schön *et al.*, *Nature* **410**, 189 (2001).
10. T. Nishino, M. Miyake, Y. Harada, U. Kawabe, *IEEE Electron Devices Lett.* **6**, 297 (1985).
11. H. Takayanagi, T. Kawakami, *Phys. Rev. Lett.* **54**, 2449 (1985).
12. A. M. Kleinsasser *et al.*, *Appl. Phys. Lett.* **55**, 1909 (1989).
13. Ch. Kloc, P. G. Simpkins, T. Siegrist, R. A. Laudise, *J. Cryst. Growth* **182**, 416 (1997).
14. Field-effect devices were prepared on the (001)-surfaces of polyacene crystals and (111)-surfaces of C_{60}, which is parallel to the molecular layers of the material.
15. J. H. Schön, S. Berg, Ch. Kloc, B. Batlogg, *Science* **287**, 1022 (2000).
16. B. D. Josephson, *Phys. Lett.* **1**, 201 (1962).
17. G. B. Arnold, *J. Low Temp. Phys.* **68**, 1 (1987).
18. K. K. Likharev, *Rev. Mod. Phys.* **51**, 101 (1979).
19. R. D. Parks, *Superconductivity* (Dekker, New York, 1969).
20. J. E. Mooij *et al.*, *Science* **285**, 1036 (1999).
21. J. E. Mooij, *Microelectron. Eng.* **47**, 3 (1999).
22. Y. Makhlin, G. Schön, A. Shnirman, *Nature* **398**, 305 (1999).
23. B. Crone *et al.*, *Nature* **403**, 521 (2000).

24. We thank L. D. Buchholz, E. A. Chandross, T. M. Klapwijk, R. de Picciotto, J. M. Rowell, and C. M. Varma for many helpful discussions, O. Schenker for technical assistance, and E. Bucher for the use of his equipment. We also thank the referees of the manuscript for their helpful comments.

5 January 2001; accepted 27 February 2001